



This is the accepted manuscript made available via CHORUS, the article has been published as:

Resummation of jet-veto logarithms in hadronic processes containing jets

Xiaohui Liu and Frank Petriello

Phys. Rev. D **87**, 014018 — Published 22 January 2013

DOI: [10.1103/PhysRevD.87.014018](https://doi.org/10.1103/PhysRevD.87.014018)

Resummation of jet-veto logarithms in hadronic processes containing jets

Xiaohui Liu, Frank Petriello

Department of Physics & Astronomy, Northwestern University, Evanston, IL 60208, USA
High Energy Physics Division, Argonne National Laboratory, Argonne, IL 60439, USA

Abstract

We derive a factorization theorem for production of an arbitrary number of color-singlet particles accompanied by a fixed number of jets at the LHC. The jets are defined with the standard anti- k_T algorithm, and the fixed number of jets is obtained by imposing a veto on additional radiation in the final state. The formalism presented here is useful for current Higgs boson analyses using exclusive jet bins, and for other studies using a similar strategy. The derivation uses the soft-collinear effective theory and assumes that the transverse momenta of the hard jets are larger than the veto scale. We resum the large Sudakov logarithms $\alpha_s^n \log^{2n-m} (p_T^J/p_T^{veto})$ up to the next-to-leading-logarithmic accuracy, and present numerical results for Higgs boson production in association with a jet at the LHC. We comment on the experimentally-interesting parameter region in which we expect our factorization formula to hold.

1 Introduction

Accurate predictions for processes with a fixed number of final-state jets are crucial for many LHC applications. A well-known example is that of a Higgs boson decaying to W -bosons at the LHC [1, 2]. The background composition to this signal changes as a function of jet multiplicity. In the zero-jet bin the background is dominated by continuum WW production, while in the one-jet and two-jet bins, top-pair production becomes increasingly important. The optimization of this search requires cuts dependent on the number of jets observed, and therefore also on theoretical predictions for exclusive jet multiplicities.

Theoretical predictions for processes with an exclusive number of jets are notoriously difficult to obtain. Fixed-order perturbation theory is plagued by large logarithms of the form $\ln(Q/p_T^{\text{veto}})$, where Q denotes the hard scale in the process, such as m_H . For experimentally relevant values $p_T^{\text{veto}} \sim 25 - 30$ GeV, residual scale variations in fixed-order calculations lead to estimated errors that do not accurately reflect uncalculated higher-order corrections [3, 4, 5]. Progress in resummation of these logarithms to all orders has been slow. Event-shape variables such as jettiness [6] allow resummation of jet-veto effects to arbitrary logarithmic accuracy, and have been applied to study the production of vector bosons or Higgs bosons plus multiple jets at the LHC [7, 11]. However, experimental measurements typically utilize jet algorithms such as the anti- k_T algorithm, and conclusions drawn from calculations using jettiness necessarily remain qualitative only. Resummation of jet-veto logarithms for the Higgs cross section in the zero-jet bin in the presence of the anti- k_T algorithm has been performed at next-to-leading logarithmic (NLL) accuracy using the semi-numerical program CAESER [5]¹. Recent work has extended these results to their NNLL accuracy [8, 9]. It has been pointed out the potentially large $\ln R$ corrections, where R is the jet-radius parameter in the anti- k_T algorithm, could have a significant numerical impact on the predictions [10]. These terms have yet to be studied at all orders and warrant further investigation.

We consider in this manuscript the resummation of the jet-veto logarithms for production of one or more color-neutral particles, such as a Higgs boson or electroweak gauge bosons, in association with one or more jets. We accomplish this by deriving a factorization theorem using soft-collinear effective theory (SCET) [14, 15, 16, 17, 18] that assumes that the transverse momenta of the hard jets are larger than the veto scale. As an example application, we consider explicitly Higgs boson production in association with a single jet. This calculation is of direct phenomenological interest for understanding the properties of the new Higgs-like state observed at the LHC [19, 20]. It extends previous work on understanding the effect of resummation on the Higgs plus zero-jet cross section [8, 9, 10]. We resum the logarithms $\ln(Q/p_T^{\text{veto}})$ through the next-to-leading logarithmic (NLL) level, where $Q \sim m_H \sim p_T^J$ and p_T^J is the transverse momentum of the observed jet. We demonstrate that the residual scale variation of the theoretical prediction is drastically reduced by the inclusion of the NLL resummation, and that the NLL+NLO result provides reliable predictions over a larger kinematic range. Since the factorization theorem we derive is valid for both more jets and

¹We note that different schemes for counting logarithms are employed in the literature; we specify in detail the order-counting scheme we use in Section 2.

other color-neutral particles, our result also serves as a framework for how to augment a host of fixed-order calculations with resummation of a class of large logarithms.

Recent work has suggested that it is difficult to extend the resummation of jet-veto logarithms in the presence of the anti- k_T algorithm beyond the NLL level [10]. We note that the logarithms appearing in the jet-vetoed cross section for Higgs plus jet production are of intermediate size; the numerical value of the leading logarithmic term in the experimentally interesting region is $\ln^2(Q/p_T^{veto}) \approx 2.5$. They are an important contribution to the cross section but do not dominate. An improved prediction requires both resummation of jet-veto logarithms and a NNLO fixed-order calculation of the process. It seems reasonable to us to first establish a factorization theorem and study the effect of resummation through the NLL level, since a NNLO calculation of the Higgs plus jet cross section is not yet available. We note that in the standard order-counting, a NNLL resummed result would also necessarily be matched with a NNLO fixed-order calculation for theoretical consistency [11].

In a more general context, there are many studies for which it would be helpful to augment fixed-order results with a NLL resummation of large logarithms to protect predictions that stray a bit too far into the wrong region of phase space, for example those that approach partonic threshold, or impose too strict a jet veto. While matching to a parton shower provides resummation of some of these effects, it is difficult to quantify the error estimate within this approach. One approach to this problem is taken in the program **CAESER** [12], which provides a semi-numerical resummation at the NLL level for many event-shape distributions at hadron colliders. The SCET framework we introduce in our manuscript allows the NLL resummation of jet-veto effects for any color-neutral particle plus multiple jets, and is easy to incorporate into a fixed-order program such as MCFM [13]. We believe that we can additionally resum threshold logarithms with a small extension of our framework. We therefore expect that the factorization theorem we establish in this manuscript will have applications beyond the Higgs plus jet process studied here.

Our paper is organized as follows. In Section 2, we derive our factorization theorem using SCET. We apply our formalism to study Higgs plus one-jet production, and discuss our numerical results, in Section 3. We conclude and discuss future directions in Section 4. All formulae needed for resummation at the NLL level are given in the Appendix.

2 Factorization and Resummation

In this section we derive a factorization theorem for multi-jet production at the LHC in the presence of a jet veto. We discuss the resummation of the logarithms associated with the jet veto through NLL accuracy. We use $pp \rightarrow \text{Higgs} + 1 \text{ jet}$ via gluon-gluon fusion as an example to highlight the derivation procedure. The generalization to additional jets is straightforward, and is presented here. Our primary results are contained in Eqs. (14), (15), (26) and (27).

2.1 Discussion of the jet constraints

We focus on the case in which the jets are defined using the hadron collider anti- k_T algorithm [21]. The following distance metrics are used:

$$\begin{aligned}\rho_{ij} &= \min(p_{T,i}^{-1}, p_{T,j}^{-1})\Delta R_{ij}/R, \\ \rho_i &= p_{T,i}^{-1}.\end{aligned}\tag{1}$$

The anti- k_T algorithm merges particles i and j to form a new particle by adding their four momenta if ρ_{ij} is the smallest among all the metrics. Otherwise, i or j is promoted to a jet depending on whether ρ_i or ρ_j is smaller, and removed from the set of considered particles. This procedure is repeated until all particles are grouped into jets. We note that $\Delta R_{ij}^2 = \Delta\eta_{ij}^2 + \Delta\phi_{ij}^2$, where $\Delta\eta_{ij}$ and $\Delta\phi_{ij}$ are the rapidity and azimuthal angle difference between particles i and j , respectively. R is the jet radius parameter and in practice is chosen to be around $0.4 - 0.5$.

After clustering the partons, we demand that the final state contains no additional jets with transverse momentum greater than a threshold p_T^{veto} . For Higgs searches, typically $p_T^{\text{veto}} \sim 25 - 30$ GeV. Since p_T^{veto} is usually substantially lower than the partonic center of mass ($\lambda \equiv p_T^{\text{veto}}/\sqrt{\hat{s}} \ll 1$), the vetoed observables are usually very sensitive to soft and collinear emissions.

Additional constraints beyond the jet veto can be imposed on the final state. In the following derivation, we require that the measured leading jets are all well-separated so that no additional small scales will be generated. We also assume that leading jet momentum $p_T^J \sim m_H \sim \sqrt{\hat{s}}$ and $1 \gg R^2 \gg \lambda^2$ while $\frac{\alpha_s}{2\pi} \log^2 R \ll 1$. The second of these requirements is necessary to insure that the measurement function factorizes into separate measurements in each of the collinear sectors. This is discussed in detail in the next section. The third requirement ensures that logarithms associated with the anti- k_T parameter R need not be resummed. Given that $p_T^{\text{veto}} \approx 25 - 30$ GeV and $R \approx 0.4 - 0.5$ for Higgs production, when the leading jet $p_T^J \approx m_H \approx 125$ GeV, these assumptions are justified.

2.2 Derivation of the factorization theorem

We use SCET [14, 15, 16, 17, 18] to establish our factorization theorem. SCET makes manifest the infrared limits of QCD by re-formulating the QCD Lagrangian using soft and collinear modes whose momenta scale with a small power-counting parameter λ in appropriate ways. For Higgs production, this parameter is of order $p_T^{\text{veto}}/\sqrt{\hat{s}}$ for radiation outside the measured jet, and is of order R for radiation inside the measured jet. Consideration of the jet algorithm and jet veto lead to the following relevant degrees of freedom in the effective theory:

- a collinear jet mode with momentum $p_J = \frac{\omega_J}{2}n_J + k_J$, where n_J is the light-cone vector along the jet direction;
- two collinear modes propagating along the beam axes a and b , with $p_i = \frac{\omega_i}{2}n_i + k_i$ for $i = a, b$;

- a soft mode with momentum k_s .

The residual momenta k_J , k_i and the soft momentum k_s all scale as $\sqrt{\hat{s}}\lambda$, while the large components of the three collinear momenta scale as $\omega_i \sim \sqrt{\hat{s}}$. We note that no ultrasoft fields ($k_{us} \sim \sqrt{\hat{s}}\lambda^2$) are needed for the process we are considering here. Any phase space measurement $\hat{\mathcal{M}}$ is assumed to be insensitive to these modes in the final state, so that $\sum_{us} \hat{\mathcal{M}}|X_{us}\rangle\langle X_{us}| = \sum_{us} |X_{us}\rangle\langle X_{us}| = 1 + \mathcal{O}(\lambda)$, where X_{us} denotes the final-state particles with an ultrasoft momentum scaling.

The leading-power SCET operator which mediates gluon-fusion Higgs plus one jet production is

$$H\mathcal{O}(x) = \sum_{\omega_i, n_i} e^{-i(\frac{\omega_1}{2}n_1 + \frac{\omega_2}{2}n_2 - \frac{\omega_3}{2}n_3)\cdot x} C_{\alpha\beta\mu}^{abc} H S_{n_1}^{aa'} S_{n_2}^{bb'} S_{n_3}^{cc'} \mathcal{B}_{\omega_1, n_1}^{\alpha, a'} \mathcal{B}_{\omega_2, n_2}^{\beta, b'} \mathcal{B}_{\omega_3, n_3}^{\mu, c'}(x), \quad (2)$$

where we have explicitly written out the Lorentz indices $\alpha\beta\mu$ and the color indices abc . H is the operator which creates a Higgs boson in the final state. $C_{\alpha\beta\mu}^{abc}$ is the hard Wilson coefficient which encodes the hard virtual fluctuations. It can be obtained order-by-order by calculating the corresponding QCD diagrams. The n -collinear gauge invariant boson field [18]

$$\mathcal{B}_{n, \omega}^\alpha = \frac{1}{g_s} [W_n^\dagger (\mathcal{P}_\perp^\alpha + g_s A_{n\perp}^\alpha) W_n] \delta_{\omega, \bar{\mathcal{P}}} \delta_{n, \hat{n}}, \quad (3)$$

which creates (annihilates) a collinear gluon in the final (initial) state, is built out of the collinear Wilson line [16]

$$W_n = \sum_{\text{perm.}} \exp \left[-g_s \frac{1}{\bar{\mathcal{P}}} \bar{n} \cdot A_n \right]. \quad (4)$$

\mathcal{P} is the projective operator acting on the collinear fields sitting to the right of it inside the parentheses. At leading power, the interactions between collinear and soft fields can be eliminated through an operator redefinition $\mathcal{B}_n^a \rightarrow S_n^{aa'} \mathcal{B}_n^{a'}$, which results in the soft Wilson line $S_n^{aa'}$ [17].

The cross section with a jet veto can be written as

$$\frac{d\sigma}{d\Phi_H} = \frac{1}{8s} \sum_{\text{spin}} \sum_X \int dx e^{-iq_H \cdot x} \langle p_a p_b | \mathcal{O}^\dagger(x) \hat{\mathcal{M}} | X_a X_b X_J X_s \rangle \langle X_s X_J X_b X_a | \mathcal{O}(0) | p_a p_b \rangle. \quad (5)$$

We have decomposed the final state into different sectors based on the momentum scaling. The operator \mathcal{O} has been written in a factorizable form, but in order to proceed, we must demonstrate that the measurement operator $\hat{\mathcal{M}}$, which includes the jet clustering operation and jet vetoing, can also be factored into different sectors up to power suppressed corrections [22]. The factorizability of the measurement operator $\hat{\mathcal{M}}$ can be seen through power-counting the anti- k_T algorithm metrics ρ_{ij} and ρ_i . Recalling that the transverse momentum p_T for each sector scales as

$$p_T^J \sim \mathcal{O}(1), \quad p_T^s \sim p_T^a \sim p_T^b \sim \mathcal{O}(\lambda), \quad (6)$$

we have

$$\begin{aligned}
\rho_{JJ} &\lesssim \rho_J \sim 1, & \rho_{Js} &\sim R^{-1}, & \rho_{Ja} &\sim \rho_{Jb} \sim R^{-1} \log \lambda^{-1}, \\
\rho_{ss} &\sim \rho_{aa} \sim \rho_{bb} \sim (\lambda R)^{-1}, & \rho_{sa} &\sim \rho_{sb} \sim \rho_{ab} \sim (\lambda R)^{-1} \log \lambda^{-1}, \\
\rho_s &\sim \rho_a \sim \rho_b \sim \lambda^{-1}.
\end{aligned} \tag{7}$$

These scalings indicate that for the jet-radius parameter R not too large ($R \ll \log \lambda^{-1}$), the contributions from the mixing between the jet and beam sectors, and the mixing between the soft and beam sectors, are power suppressed. Jets tend to form separately within each sector. As long as $R \ll 1$, radiation collinear to the jet direction will be combined before it is clustered with soft radiation. This means that the soft radiation is insensitive to the details of the collinear radiation except for the jet direction. Therefore, $\hat{\mathcal{M}}$ can also be factored between these two sectors. The measurement operator can therefore be factored as

$$\hat{\mathcal{M}} = \hat{\mathcal{M}}_J \hat{\mathcal{M}}_s \hat{\mathcal{M}}_a \hat{\mathcal{M}}_b, \tag{8}$$

up to power-suppressed corrections in p_T^{veto} and R . The individual \mathcal{M}_A will be given in the Appendix.

Plugging in the definition of the operator \mathcal{O} , the cross section can be written as

$$\begin{aligned}
\frac{d\sigma}{d\Phi_H} &= \frac{1}{8s} \sum_{spin} \sum_{n_A} \int d\omega_A \int dx e^{i(\frac{\omega_a}{2} n_a + \frac{\omega_b}{2} n_b - \frac{\omega_J}{2} n_J - q_H) \cdot x} \\
&\times C_{\alpha\beta\mu}^{abc\dagger} C_{\alpha'\beta'\mu'}^{a'b'c'} \sum_{X_s} \langle 0 | S_{n_a}^{aa_1} S_{n_b}^{bb_1} S_{n_J}^{cc_1}(x) | X_s \rangle \langle X_s | S_{n_a}^{a'_1 a'} S_{n_b}^{b'_1 b'} S_{n_J}^{c'_1 c'}(0) | 0 \rangle \\
&\times \sum_{X_a} \langle p_a | \mathcal{B}_{n_a}^{\alpha, a_1}(x_{n_a}^-, x_{n_a}^\perp, 0_{n_a}) | X_a \rangle \langle X_a | \delta(\omega_a - \bar{\mathcal{P}}_a) \delta_{n_a, \hat{n}_a} \mathcal{B}_{n_a}^{\alpha', a'_1}(0) | p_a \rangle \\
&\times \sum_{X_b} \langle p_b | \mathcal{B}_{n_b}^{\beta, b_1}(x_{n_b}^-, x_{n_b}^\perp, 0_{n_b}) | X_b \rangle \langle X_b | \delta(\omega_b - \bar{\mathcal{P}}_b) \delta_{n_b, \hat{n}_b} \mathcal{B}_{n_b}^{\beta', b'_1}(0) | p_b \rangle \\
&\times \sum_{n_J} \sum_{X_J} \langle 0 | \mathcal{B}_{n_J}^{\mu, c_1}(x_{n_J}^-, x_{n_J}^\perp, 0_{n_J}) | X_J \rangle \langle X_J | \delta(\omega_J - \bar{\mathcal{P}}_J) \delta_{n_J, \hat{n}_J} \mathcal{B}_{n_J}^{\mu', c'_1}(0) | 0 \rangle. \tag{9}
\end{aligned}$$

Here, \sum'_X means summing over the final states with the restrictions imposed by $\hat{\mathcal{M}}$. We have suppressed $\hat{\mathcal{M}}$ for simplicity. In the last line, \sum_{n_J} indicates the need to sum over all possible directions of different n_J -jet modes. We have removed several Kronecker-deltas using the discrete sums. The remaining ones have been turned into integrals $\int d\omega_A$ and delta functions $\delta(\omega_A - \bar{\mathcal{P}}_A)$, after combining the residual momentum $k_{n_A}^- \equiv \bar{n}_A \cdot k_A$ with the label momentum ω_A in the collinear sector A for $A = a, b, J$. We note that the collinear sectors do not depend on $x_A^+ \equiv n_A \cdot x$.

We further modify this expression by performing a translational operation in each sector and inserting several residual momentum operators $\int dk \delta(k - \hat{k})$ to remove the explicit

momentum dependence on the final states. This gives us

$$\begin{aligned}
\frac{d\sigma}{d\Phi_H} &= \frac{1}{8s} \sum_{spin} \sum_{n_A} \int d\omega_A \int dx \int d^4k_s \int d\mathbf{k}_A e^{i(\frac{\omega_a}{2}n_a + \frac{\omega_b}{2}n_b - \frac{\omega_J}{2}n_J - q_H - k_s + \mathbf{k}_a + \mathbf{k}_b - \mathbf{k}_j) \cdot x} \\
&\quad \times C_{\alpha\beta\mu}^{abc\dagger} C_{\alpha'\beta'\mu'}^{a'b'c'} \sum_{X_s} \langle 0 | S_{n_a}^{aa_1} S_{n_b}^{bb_1} S_{n_J}^{cc_1} (0) | X_s \rangle \langle X_s | \delta^4(k_s - \hat{k}_s) S_{n_a}^{a'_1 a'} S_{n_b}^{b'_1 b'} S_{n_J}^{c'_1 c'} | 0 \rangle \\
&\quad \times \sum_{X_a} \langle p_a | \mathcal{B}_{n_a}^{\alpha, a_1} (0) | X_a \rangle \langle X_a | \delta(k_a^+ - \hat{k}_a^+) \delta^2(k_a^\perp - \hat{k}_a^\perp) \delta(\omega_a - \bar{\mathcal{P}}_a) \delta_{n_a, \hat{n}_a} \mathcal{B}_{n_a}^{\alpha', a'_1} (0) | p_a \rangle \\
&\quad \times \sum_{X_b} \langle p_b | \mathcal{B}_{n_b}^{\beta, b_1} (0) | X_b \rangle \langle X_b | \delta(k_b^+ - \hat{k}_b^+) \delta^2(k_b^\perp - \hat{k}_b^\perp) \delta(\omega_b - \bar{\mathcal{P}}_b) \delta_{n_b, \hat{n}_b} \mathcal{B}_{n_b}^{\beta', b'_1} (0) | p_b \rangle \\
&\quad \times \sum_{X_J} \langle 0 | \mathcal{B}_{n_J}^{\mu, c_1} (0) | X_J \rangle \langle X_J | \delta(k_J^+ - \hat{k}_J^+) \delta^2(k_J^\perp - \hat{k}_J^\perp) \delta(\omega_J - \bar{\mathcal{P}}_J) \mathcal{B}_{n_J}^{\mu', c'_1} (0) | 0 \rangle, \quad (10)
\end{aligned}$$

where $d\mathbf{k} \equiv dk^+ d^2k^\perp$. We now drop all residual momenta of order λ or higher, keeping homogeneously only the leading power terms in the exponent (dropping the contributions of order λ means that we ignore the recoil effect in the transverse plane). We perform the integration over the k_A^+ component in each collinear sector to indicate that no restrictions are applied on this residual momentum². This leads to

$$\begin{aligned}
\frac{d\sigma}{d\Phi_H} &= \frac{1}{8s} \sum_{spin} \int d\omega_A \sum_{n_J} d^2k_J^\perp (2\pi)^4 \delta^4\left(\frac{\omega_a}{2}n_a + \frac{\omega_b}{2}n_b - \frac{\omega_J}{2}n_J - q_H\right) \\
&\quad \times C_{\alpha\beta\mu}^{abc\dagger} C_{\alpha'\beta'\mu'}^{a'b'c'} \int d^4k_s \langle 0 | S_{n_a}^{aa_1} S_{n_b}^{bb_1} S_{n_J}^{cc_1} (0) \hat{\mathcal{M}}_s \delta^4(k_s - \hat{k}_s) S_{n_a}^{a'_1 a'} S_{n_b}^{b'_1 b'} S_{n_J}^{c'_1 c'} | 0 \rangle \\
&\quad \times \int d^2k_a^\perp \langle p_a | \mathcal{B}_{n_a}^{\alpha, a_1} (0) \hat{\mathcal{M}}_a \delta^2(k_a^\perp - \hat{k}_a^\perp) \delta(\omega_a - \bar{\mathcal{P}}_a) \mathcal{B}_{n_a}^{\alpha', a'_1} (0) | p_a \rangle \\
&\quad \times \int d^2k_b^\perp \langle p_b | \mathcal{B}_{n_b}^{\beta, b_1} (0) \hat{\mathcal{M}}_b \delta^2(k_b^\perp - \hat{k}_b^\perp) \delta(\omega_b - \bar{\mathcal{P}}_b) \mathcal{B}_{n_b}^{\beta', b'_1} (0) | p_b \rangle \\
&\quad \times \langle 0 | \mathcal{B}_{n_J}^{\mu, c_1} (0) \hat{\mathcal{M}}_J \delta^2(k_J^\perp - \hat{k}_J^\perp) \delta(\omega_J - \bar{\mathcal{P}}_J) \mathcal{B}_{n_J}^{\mu', c'_1} (0) | 0 \rangle. \quad (11)
\end{aligned}$$

To reach the formula above, we have summed over the final states using $\sum_X |X\rangle\langle X| = 1$ and have re-inserted the measurement operators $\hat{\mathcal{M}}_A$. We next define the beam and the jet functions

$$\begin{aligned}
f_{\perp g/p}(z, p_T^{veto}, R) &= \int d^2k^\perp \sum_{spin} -\omega \langle p | \mathcal{B}_n^{\alpha, a} (0) \hat{\mathcal{M}}_B \delta^2(k^\perp - \hat{k}^\perp) \delta(\omega - \bar{\mathcal{P}}) \mathcal{B}_{n, \alpha, a} (0) | p \rangle, \\
J(R) g_{\perp}^{\mu\mu'} \delta^{cc'} &= 2(2\pi)^3 (-\omega_J) \langle 0 | \mathcal{B}_{n_J}^{\mu, c} (0) \hat{\mathcal{M}}_J \delta^2(k_J^\perp - \hat{k}_J^\perp) \delta(\omega_J - \bar{\mathcal{P}}_J) \mathcal{B}_{n_J}^{\mu', c'} (0) | 0 \rangle, \quad (12)
\end{aligned}$$

²We note that this assumes that no pseudorapidity cut is imposed on the observed low p_T jet. It is straightforward to remove this constraint if desired; for simplicity of presentation we do not do so here.

and the soft function

$$S(\mathbf{n}_J, R, p_T^{veto}) = \int d^4 k_s \langle 0 | S_{n_a}^{aa_1} S_{n_b}^{bb_1} S_{n_J}^{cc_1}(0) \hat{\mathcal{M}}_s \delta^4(k_s - \hat{k}_s) S_{n_a}^{a_1 a'} S_{n_b}^{b_1 b'} S_{n_J}^{c_1 c'}(0) | 0 \rangle. \quad (13)$$

We emphasize that the beam and jet functions are well-defined only after the soft zero-bin subtraction has been properly performed [25].

Finally, we arrive at our result

$$\begin{aligned} d\sigma &= d\Phi_H d\Phi_J \int dx_a dx_b \frac{1}{2\hat{s}} \frac{1}{4} \left(\frac{1}{N_c^2 - 1} \right)^2 (2\pi)^4 \delta^4(q_a + q_b - q_J - q_H) \\ &\quad \times \text{Tr}(H \cdot S) f_{\perp g/p_a}(x_a, p_T^{veto}, R) f_{\perp g/p_b}(x_b, p_T^{veto}, R) J(R), \end{aligned} \quad (14)$$

with the help of identifying $\sum_n \frac{1}{2(2\pi)^3 \omega_J} d\omega_J d^2 k_J^\perp$ as the massless particle phase space $d\Phi_J = \frac{\bar{q}_J}{8(2\pi)^3} dq_J d\Omega$. We define the hard function $H \equiv CC^\dagger$. The trace is over the color indices. Since p_T^{veto} is much larger than Λ_{QCD} , the beam function can be further matched onto parton distribution functions at the beam scale $\mu_B \sim p_T^{veto}$: $f_{i,\perp} = \mathcal{I}_{ij} \otimes f_j(x)$. The matching coefficient \mathcal{I}_{ij} can be calculated perturbatively. We have chosen our normalization so that at leading order, $\mathcal{I}_{ij} = \delta(1-x)\delta_{ij}$, $J(R) = 1$ and $S = \delta^{aa'}\delta^{bb'}\delta^{cc'}$. The factorization reproduces the tree-level $gg \rightarrow Hg$ cross section. We note that for NLL resummation, only the leading-order matching coefficients are needed. In the Appendix, we will present the NLO results for the jet and beam functions, up to $\mathcal{O}(R)$ corrections.

The formalism is easily generalized to processes with an arbitrary number of jets and non-strongly interacting particles in the final state. All the arguments go through identically. We find

$$\begin{aligned} d\sigma &= d\Phi_{H_c} d\Phi_{J_i} \mathcal{F}(\Phi_{H_c}, \Phi_{J_i}) \sum_{a,b} \int dx_a dx_b \frac{1}{2\hat{s}} (2\pi)^4 \delta^4 \left(q_a + q_b - \sum_i^n q_{J_i} - \sum_c q_{H_c} \right) \\ &\quad \times \sum_{\text{spin}} \sum_{\text{color}} \text{Tr}(H \cdot S) \mathcal{I}_{a,i_a j_a} \otimes f_{j_a}(x_a) \mathcal{I}_{b,i_b j_b} \otimes f_{j_b}(x_b) \prod_i^n J_{J_i}(R), \end{aligned} \quad (15)$$

where $d\Phi_{H_c}$ and $d\Phi_{J_i}$ denote the phase space measures for the color neutral particle H_c and the massless jets J_i , respectively. $\mathcal{F}(\Phi_{H_c}, \Phi_{J_i})$ includes all additional phase-space cuts other than the p_T veto acting on H_c and the n hard jets, which should guarantee well separated n -jet final states ($n_{J_i} \cdot n_{J_j} \gg \lambda$). The measured jet p_T^J should be much larger than p_T^{veto} .

We note that possible issues arise when attempting to extend the resummation to the NNLL level, as pointed out in Ref. [10]. For $R \gg \lambda$, corrections of the form

$$\alpha_s^2 R^2 \ln \lambda \quad (16)$$

appear, which prohibit soft-collinear factorization. In the limit $R \sim \lambda$, clustering logarithms of the form

$$\alpha_s^2 \ln R \ln \lambda \quad (17)$$

which prohibit even NLL resummation occur. Let us study the numerical impact of these terms for the parameter values relevant for Higgs production. Setting $R = 0.4$, $m_H = 126$ GeV, and $p_T^{veto} = 25$ GeV, we find $R^2 = 0.16$, $\ln(1/\lambda) = 1.6$, and $\ln(1/R) = 0.92$. For $R = 0.5$, $\ln(1/R) = 0.69$. It is clear that the corrections of Eq. (16) are indeed power-suppressed for experimentally-relevant value of $R \approx 0.4 - 0.5$. They can be obtained to sufficient accuracy by matching to fixed-order results. There is also a hierarchy $\ln(1/\lambda) > \ln(1/R)$; the clustering logarithms are not large for relevant jet parameters. An eventual inclusion of the leading clustering effects by combining the resummation with a NNLO calculation of Higgs plus one-jet production should be sufficient. We therefore believe that it makes sense to study the resummation of jet-veto logarithms in Higgs production, and proceed with our analysis.

We also comment briefly on the validity of our effective-theory approach before continuing. There are two distinct regions of phase space that contribute to $pp \rightarrow \text{Higgs} + \text{jet}$: (1) $m_H \sim p_T^J \gg p_T^{veto}$, and (2) $m_H \gg p_T^J \sim p_T^{veto}$. Other parameter hierarchies can be obtained as limits of these two regions. Our EFT approach captures all large logarithms in the first region; we resum all logarithms of the form $\ln(Q/p_T^{veto})$, where $Q \sim m_H \sim p_T^J$. In the other region with $p_T^J \sim p_T^{veto}$, we do not correctly capture the large logarithms. We do as well (or as badly) as a fixed-order calculation. A different EFT is needed for this region, and this will be the subject of future work. We note that depending on the exact definition of region (1), it contributes between 30-50% of the total Higgs+jet cross section, so it is a significant fraction of the full result.

2.3 NLL Resummation

Each ingredient in Eqs. (14) and (15) describes fluctuations with a particular momentum scaling. When the hard, jet, beam and soft functions are calculated near their natural scales, no large logarithms will arise. The typical scales for each sector are

$$\mu_H \sim p_T^J, \quad \mu_J \sim p_T^J R, \quad \mu_B \sim \mu_S \sim p_T^{veto}. \quad (18)$$

However, calculating the cross section requires all the functions to be evaluated at the same factorization scale μ , which generates large logarithms of the following ratios:

$$\frac{p_T^J}{\mu}, \quad \frac{p_T^J R}{\mu}, \quad \frac{p_T^{veto}}{\mu}. \quad (19)$$

These large logarithms can be resummed by evolving each function to the scale μ using the renormalization group (RG) equation

$$\mu \frac{dF}{d\mu} = \gamma_\mu(\mu) F(\mu). \quad (20)$$

The anomalous dimension γ_μ can be extracted most easily from the ϵ poles of each function calculated using dimensional regularization.

However, like for small- q_T resummation, a subtlety arises because of the identical virtuality shared by the collinear and soft degrees of freedom [25, 26]. Various efforts have been made in SCET to regulate this rapidity divergence [26, 27, 28], which all have shown to be able to reproduce correctly the NLO fixed-order QCD singularities. In our current approach, we adopt the formalism proposed in Ref. [26]. We regulate the extra divergence by modifying the collinear and the soft Wilson lines as follows:

$$\begin{aligned} W_n &\rightarrow \sum_{\text{perm.}} \exp \left(-g_s \frac{1}{\bar{\mathcal{P}}} \left[w^2 \frac{|\bar{\mathcal{P}}|^{-\eta}}{\nu^{-\eta}} \bar{n} \cdot A_n \right] \right), \\ S_n &\rightarrow \sum_{\text{perm.}} \exp \left(-g_s \frac{1}{\mathcal{P}} \left[w \frac{|2\mathcal{P}^3|^{-\eta/2}}{\nu^{-\eta/2}} n \cdot A_s \right] \right), \end{aligned} \quad (21)$$

where the bookkeeping parameter w will be set to 1 as $\eta \rightarrow 0$. The effective rapidity cut-off ν and the new parameter η play similar roles as μ and ϵ in dimensional regularization. The corresponding rapidity-RG equation commutes with the conventional one for the beam and the soft functions: $[\mu \frac{\partial}{\partial \mu}, \nu \frac{\partial}{\partial \nu}] = 0$,

$$\nu \frac{dF_{B,S}}{d\nu} = \gamma_\nu(\nu) F_{B,S}(\nu). \quad (22)$$

The natural ν -scale choices for the beam and the soft functions are

$$\nu_B \sim x_{a,b} \sqrt{s}, \quad \nu_S \sim p_T^{\text{veto}}. \quad (23)$$

Since the physical cross section is μ and ν independent, the anomalous dimensions must obey the consistency conditions

$$\begin{aligned} 2\gamma_H^\mu + \gamma_J^\mu + \gamma_B^\mu + \gamma_S^\mu &= 0, \\ \gamma_B^\nu + \gamma_S^\nu &= 0, \end{aligned} \quad (24)$$

up to power corrections of order λ and effects due to finite jet (beam) separations [23]. We will use these conditions to extract the anomalous dimension for the soft function. The general solution to the RG equation can be formally written as

$$F(\mu, \nu) = U(\mu, \nu, \mu_0, \nu_0) F(\mu_0, \nu_0). \quad (25)$$

The explicit form of the evolution kernel U for each function along with all details needed for NLL resummation are given in the Appendix.

Recalling that for NLL resummation only the tree-level Wilson coefficients are needed, we find the following simplified expression for production of a color-neutral particle plus one jet:

$$\begin{aligned} d\sigma_{\text{NLL}} &= \sum_{ab} \int d\hat{\sigma}_{\text{LO}}^{ab \rightarrow hk}(\mu_H, x_a, x_b) f_a(\mu_B, x_a) f_b(\mu_B, x_b) \\ &\quad \times U_{H,k}(\mu, \mu_H) U_{S,k}(\mu, \nu, \mu_S, \nu_S) \mathcal{I}_{B,a,b}(\mu, \nu, \mu_B, \nu_B, x_a, x_b) \mathcal{R}_J(\mu, \mu_J, R). \end{aligned} \quad (26)$$

For a more general process, the evolutions of the hard and the soft functions will usually induce operator mixing in color space. Therefore, the NLL cross section for multi-jet production reads

$$\begin{aligned}
d\sigma_{\text{NLL}} = & \sum_{ab} \int dx_a dx_b \text{Tr} \left[H_{\text{LO}}^{ab \rightarrow h_c \{k\}}(\mu_H) S U_{H, \{k\}}(\mu, \mu_H) U_{S, \{k\}}(\mu, \nu, \mu_S, \nu_S) \right] \\
& \times f_a(\mu_B, x_a) f_b(\mu_B, x_b) \mathcal{I}_{B, a, b}(\mu, \nu, \mu_B, \nu_B, x_a, x_b) \prod_i \mathcal{R}_{J_i}(\mu, \mu_{J_i}, R). \quad (27)
\end{aligned}$$

We note that due to the separation between the scales inside and outside the allowed jets, a full refactorization or a refactorization ansatz of the soft function [23, 24] may be helpful in improving the resummation accuracy. Since this involves $\ln R$ effects and is therefore moderate for the experimentally-interesting p_T^{veto} and R , it will be left for further studies. There also exist non-global logarithms [29] beginning at the NLL' level according to the order-counting of Ref. [11], whose resummation is beyond the scope of our formalism presented in this work.

Different schemes are used in the literature to determine the accuracy of resummation prescriptions. When calling our result NLL, we use the order-counting defined in Ref. [11]. This means that we include the two-loop cusp anomalous dimension, and the one-loop non-cusp anomalous dimensions for the beam, soft, jet and hard functions. We therefore achieve NLO accuracy in the exponent of the Sudakov form factor. Our beam, soft, jet and hard functions are taken to be leading-order. Denoting the large logarithms associated with the veto scale generically as L , our NLL captures the two leading logarithms at each order in α_s . We correctly obtain $\alpha_s L^2$ and $\alpha_s L$, $\alpha_s^2 L^4$ and $\alpha_s^2 L^3$, $\alpha_s^3 L^6$ and $\alpha_s^3 L^5$, and so on. To obtain the next tower of logarithms ($\alpha_s^2 L^2$, $\alpha_s^3 L^4$, etc.), we would need to include the jet, beam and soft functions at 1-loop. This would correspond to NLL' in the language of Ref. [11], or to the NLL implied in the traditional QCD approach [5]. All ingredients are currently known for this extension except for the one-loop soft function, which is not difficult to obtain. We plan to include this term in future detailed numerical studies. Control over the next tower of logarithms ($\alpha_s^2 L$, $\alpha_s^3 L^3$, etc.) would require the two-loop non-cusp anomalous dimensions γ_x , and would correspond to NNLL in the notation of Ref. [11]. We note that since we match to the full NLO result from MCFM, we should in principle include the hard, beam, jet and soft functions also to NLO accuracy in order to maintain theoretical consistency in the powers of α_s included. We will correct this shortcoming in future work.

3 Numerical results for Higgs+jet production

We present in this section numerical results for $pp \rightarrow h + \text{jet}$ at an 8TeV LHC with a jet veto imposed. We combine our resummation with the NLO cross section from MCFM to produce NLL+NLO results. In the numerics presented here we restrict the leading jet rapidity to $|\eta_J| < 2.5$ and veto all other jets with $p_{T, i} > p_T^{\text{veto}}$ and $|\eta_i| < \infty$ for simplicity. Experiments typically only veto jets in the range $|\eta| \lesssim 4.5$. However, we expect that this boundary effect will be small [5]. It is simple to include this constraint if desired, as discussed in the previous

section. We have included the gg , qg , and $q\bar{q}$ partonic scattering channels in obtaining these results. All relevant beam, jet and soft functions, as well as anomalous dimensions needed for this calculation, are presented in the Appendix.

We begin by demonstrating that our formalism correctly sums all the next-to-leading logarithms of p_T^{veto}/p_T^J by comparing the expanded NLL production rate with the MCFM NLO result [13]. In the expanded NLL result, we have included the large non-logarithmic virtual corrections by using the full NLO hard function taken from Ref. [30]. The validity of our formalism is shown in Fig. 1, where we show the agreement between these two results in the region where $\log p_T^J/p_T^{veto}$ becomes large. This demonstration is based on the dominance of the log terms over the other contributions omitted in SCET in the small p_T^{veto} region.

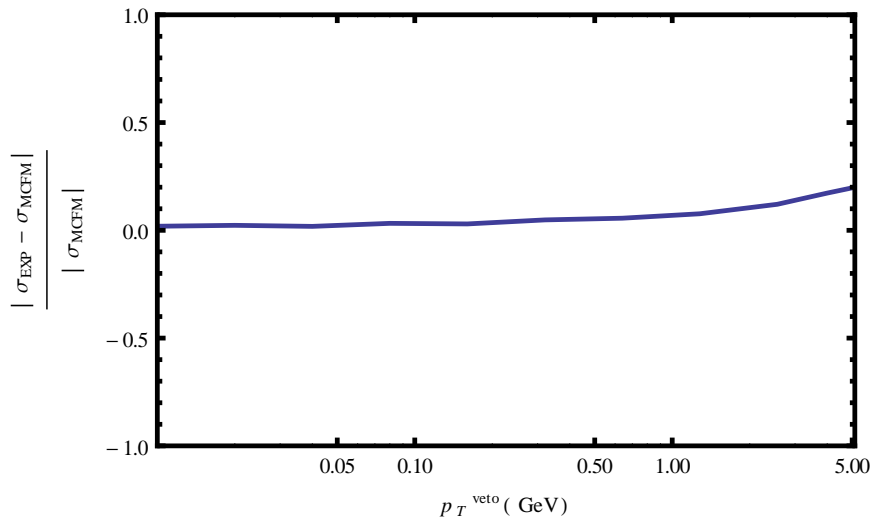


Figure 1: Presented is the ratio of the expanded SCET cross section $|\sigma_{\text{exp}}|$ and the full NLO QCD calculation from MCFM σ_{MCFM} , $|\sigma_{\text{exp}} - \sigma_{\text{MCFM}}|/|\sigma_{\text{MCFM}}|$. We have required the leading jet $p_T^J > 120\text{GeV}$, $|\eta_J| < 2.5$, have set $R = 0.1$ and have made p_T^{veto} as low as 0.01GeV . The excellent agreement between the expanded SCET prediction and the MCFM cross section for such low p_T^{veto} implies that our formalism catches all the NLL structures.

We next study the cross section for Higgs+jet production. Since Eq. (26) is only valid for $p_T^{veto} \ll p_T^J$, in order to give a prediction over the entire allowed kinematic range, we have to combine the resummed formula of Eq. (26) with the full NLO result. For this purpose, we adopt the matching scheme proposed in Ref. [5], in which the RG-improved cross section is taken as

$$\sigma = \left(\frac{\sigma_{\text{NLL}}}{\sigma_{\text{LO}}} \right)^Z \left[\sigma_{\text{NLO}}(\mu) - Z (\sigma_{\text{exp}}(\mu) - \sigma_{\text{LO}}(\mu)) \right], \quad (28)$$

where $Z = (1 - p_T^{veto}/p_T^{max})$. σ_{LO} is the LO cross section and σ_{NLO} is the cross section calculated through NLO using MCFM. σ_{exp} is obtained by expanding the resummed cross section σ_{NLL} in Eq. (26). We postpone rigorous study of the uncertainty induced by the

choice of matching procedure to future work. In evaluating the resummed production rate σ_{NLL} , we fix

$$\begin{aligned}\mu_H &= \left[(x_a \sqrt{s})^{T_a \cdot T_a} (x_b \sqrt{s})^{T_b \cdot T_b} (p_T^J)^{T_J \cdot T_J} \right]^{\frac{1}{\sum_i T_i \cdot T_i}}, \\ \mu_J &= p_T^J R, \\ \mu_B = \mu_S &= p_T^{\text{veto}}.\end{aligned}\tag{29}$$

These choices minimize the logarithmic dependence in the hard, jet and the beam functions. When we use this set of scale choices, the cross section is also independent of the rapidity scale ν .

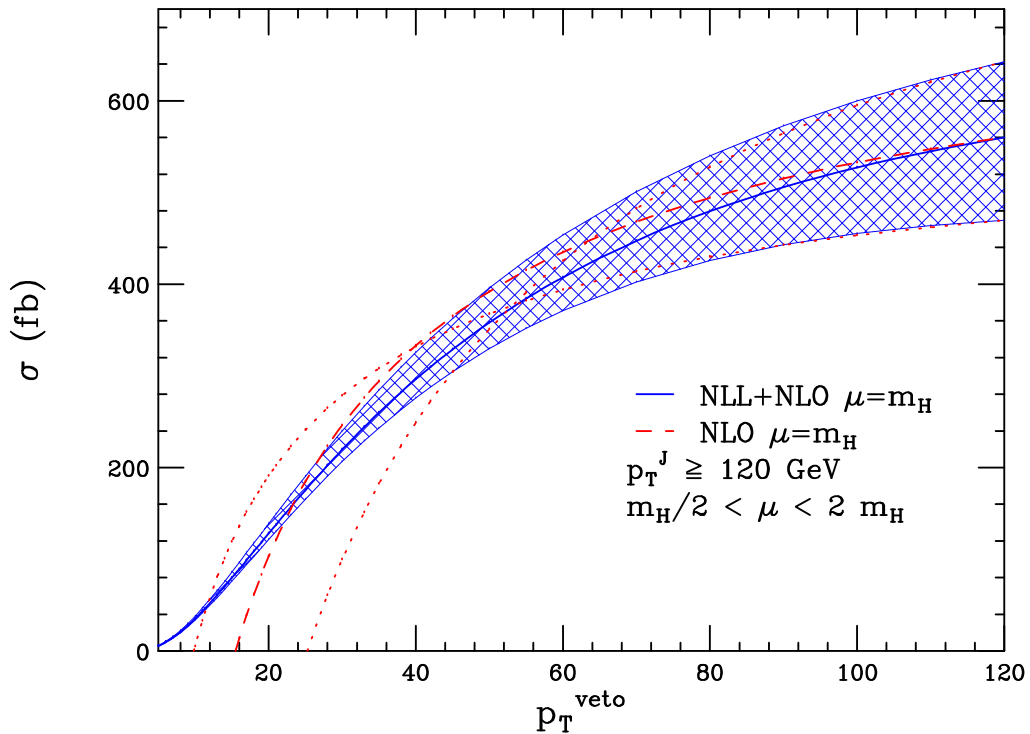


Figure 2: Shown are the NLO+NLL prediction and the NLO cross section as a function of p_T^{veto} for $p_T^J \geq 120$ GeV. The solid-blue curve represents the RG-improved cross section in Eq. (28). The dashed-red line shows the NLO result for the scale choice $\mu = m_H$, while the dotted red lines show the NLO result for $\mu = m_H/2$ and $\mu = 2m_H$. The blue band reflects the scale uncertainty of the RG-improved rate. The band boundaries are set by the values at the scale choices $m_H/2$ and $2m_H$.

In Fig. 2, we demonstrate the improvement obtained with NLL resummation by showing the dependence of both the NLO and RG-improved integrated cross sections on different choices of p_T^{veto} . We have set $p_T^J > 120\text{GeV}$, $\mu = m_H = 126\text{GeV}$ and have taken the anti- k_T parameter $R = 0.4$. For the matching in Eq. (28), we use $p_{T,veto}^{max} = 120\text{ GeV}$ in Z . We use the MSTW2008 NLO PDF set [31] with two-loop α_s running. We can see that for small values of p_T^{veto} , the fixed-order cross section becomes negative while the NLO + NLL result remains positive. We also vary the scale μ from $m_H/2$ to $2m_H$ to estimate the theoretical uncertainty. We can see that resumming the large logarithms greatly reduces the residual scale variation for the experimentally relevant values $p_T^{veto} \approx 25 - 30\text{ GeV}$, leading to a more reliable prediction. The fixed-order cross section exhibits little scale variation for $p_T^{veto} \approx 55\text{ GeV}$. Similar behavior is observed for the Higgs plus zero-jet cross section [3, 4], and was argued to result from an accidental cancellation between several higher-order corrections with different origins. The same argument holds here for the Higgs plus one-jet result. As p_T^{veto} becomes large, the fixed-order and resummed cross section coincide. Since the separation between the hard scale and p_T^{veto} vanishes in this limit, this behavior is expected.

To gain some intuition regarding how low in p_T^J the resummation of jet-veto logarithms leads to a difference from fixed-order, we fix $p_T^{veto} = 25\text{ GeV}$ and integrate over the leading-jet transverse momentum subject to the constraint $p_T^J \geq p_{T,min}^j$. We stress that some caution must be exercised in using these results. Our effective theory framework is only valid when the hierarchy $p_T^{veto} \ll p_T^J$ exists. When $p_T^{veto} \sim p_T^J$, our result reduces to the fixed-order result, which contains the ratio of scales $p_T^{veto} \ll m_H$. A different effective theory framework consisting is needed to resum logarithms of this ratio. With these caveats stated, we plot in Fig. 3 the NLO and NLL+NLO results as a function of the minimum allowed jet p_T for $p_T^{veto} = 25\text{ GeV}$. Significant differences between both the central values and residual scale uncertainties persist down to low values of p_T^{min} , indicating the need to augment the fixed-order results with resummation over the entire p_T^J region.

4 Conclusions

In this manuscript, we have established a formalism for the production of color-singlet particles produced in association with an exclusive number of jets at the LHC. Using effective field theory techniques, we have proven the factorization theorem of Eqs. (14) and (15), which allows us to resum large Sudakov logarithms of the form $\log p_T^{veto}/Q$ with $Q \sim m_H \sim p_T^J$ to all orders. We have focused on Higgs production in association with a jet as an example. We have demonstrated by the excellent agreement between the expanded NLL result and NLO QCD cross section that our formalism correctly captures all relevant large logarithms in the $p_T^{veto}/Q \rightarrow 0$ limit. The scale uncertainty of the cross section is greatly reduced by inclusion of the resummation. By matching our results with MCFM, we provide a NLL+NLO result for Higgs+jet production valid over the entire kinematic range. With our results, it is easy to supplement fixed-order results for vector boson or Higgs boson production with the resummation of jet-veto logarithms in order to provide predictions valid throughout phase space.

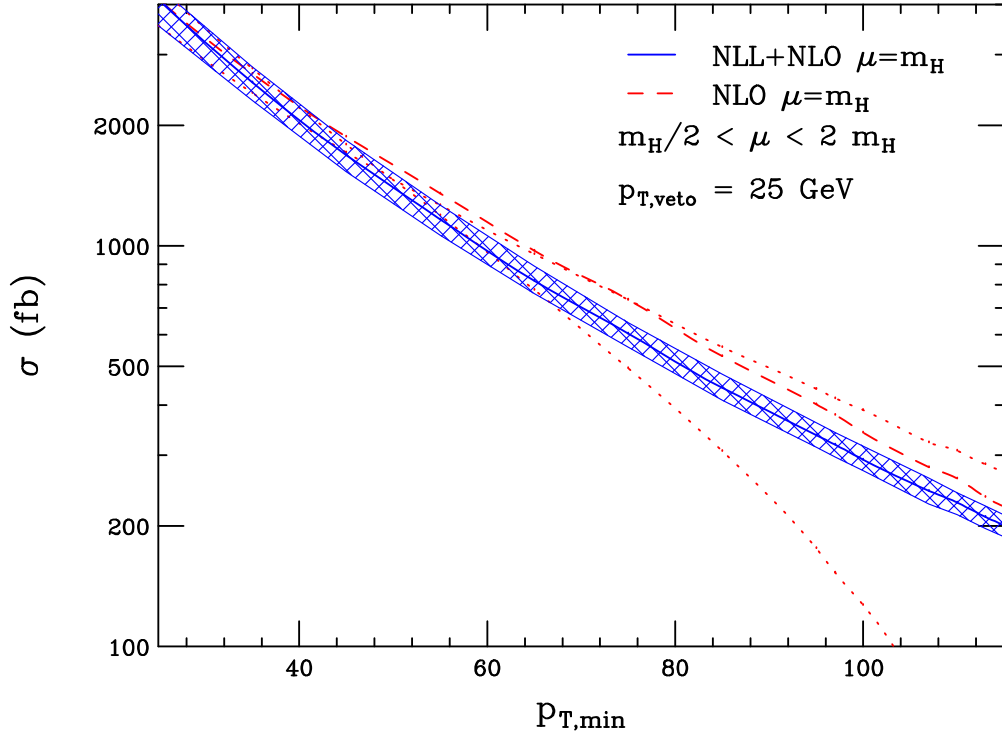


Figure 3: The NLO+NLL prediction and the NLO cross section as a function of p_T^{min} for $p_T^{veto} = 25\text{GeV}$. The solid-blue curve represents the RG-improved cross section in Eq. (28). The dashed-red line shows the NLO result for the scale choice $\mu = m_H$, while the dotted red lines show the NLO result for $\mu = m_H/2$ and $\mu = 2m_H$. The blue band reflects the scale uncertainty of the RG-improved rate. The band boundaries are set by the values at the scale choices $m_H/2$ and $2m_H$.

Several future directions remain to be pursued. With our results it is possible to improve the theoretical predictions for Higgs plus one or two jets. This will be of great phenomenological importance as the properties of the new state discovered at the LHC are further analyzed. We plan to further investigate these phenomenological application of our formalism. It is also interesting to study the effective theory valid when both the veto scale and the leading jet p_T are smaller than m_H . Beyond NLL', extra clustering effects will enter the cross section, which are not completely understood [10] yet. We have argued that the numerical impact of these terms should be subdominant to the effects studied here. However, a NNLO calculation of the jet, beam and soft functions would be helpful in determining whether this formalism can be extended beyond NLL'. In the current work, we have simpli-

fied the calculation of the anti- k_T jet function by keeping the leading R contributions only in the resummation formulae. It will be phenomenologically interesting to include higher order corrections in R to improve the accuracy. We have also neglected for simplicity the boundary effects due to the experimentally finite η range. These issues will be addressed in future detailed phenomenological studies.

Acknowledgments

We thank Kirill Melnikov, Jui-yu Chiu, Sonny Mantry, Markus Schulze, Jonathan Walsh, Frank Tackmann and Giulia Zanderighi for helpful discussions. We thank Joey Huston for pointing out a numerical bug in Fig. 3 in the previous version of this work. This work is supported by the U.S. Department of Energy, Division of High Energy Physics, under contract DE-AC02-06CH11357 and the grants DE-FG02-95ER40896 and DE-FG02-08ER4153.

A Fixed-order jet and beam functions

In this Appendix, we list all ingredients needed for NLL resummation. We start with the NLO calculation of the jet and the beam functions, whose definitions can be found in Eq. (12). The anti- k_T jet function is calculated using the measurement function

$$\hat{\mathcal{M}}_J = \Theta(\Delta\eta_{ij}^2 + \Delta\phi_{ij}^2 < R^2) + \mathcal{O}(p_T^{veto}). \quad (30)$$

We explicitly calculate that the jet collinear radiation leaking outside the jet is power-suppressed by p_T^{veto} after correctly subtracting the soft zero-bin contributions. Since numerically $R \ll 1$, we can simplify the measure using

$$\Delta\eta_{ij}^2 + \Delta\phi_{ij}^2 = 2 \cosh(\Delta\eta_{ij}) - 2 \cos(\Delta\phi_{ij}) + \mathcal{O}(R^4). \quad (31)$$

In this limit, the NLO jet functions for gluons and quarks become

$$\begin{aligned} J_g^{(1)} &= \frac{\alpha_s(\mu)}{2\pi} \left[C_A \left(\frac{67}{9} - \frac{3\pi^2}{4} \right) - \frac{23}{9} \frac{n_f}{2} + \beta_0 \log \frac{\mu}{p_T^J R} + 2C_A \log^2 \frac{\mu}{p_T^J R} \right] + \mathcal{O}(R^2), \\ J_q^{(1)} &= \frac{\alpha_s(\mu)}{2\pi} C_F \left[\frac{13}{2} - \frac{3\pi^2}{4} + 3 \log \frac{\mu}{p_T^J R} + 2 \log^2 \frac{\mu}{p_T^J R} \right] + \mathcal{O}(R^2). \end{aligned} \quad (32)$$

The measure for the beam function with one emission is

$$\hat{\mathcal{M}}_B = \Theta(k_{T,i} < p_T^{veto}) \Theta(|\eta_i| < \eta_{\text{cut}}) + \Theta(|\eta_i| > \eta_{\text{cut}}). \quad (33)$$

Experimentally, $\eta_{\text{cut}} \sim 4.5$. For simplicity, we set $\eta_{\text{cut}} = \infty$ here. We note that this difference does not affect the anomalous dimension of the beam function, it only changes the finite

part. The calculation is performed using the 't Hooft-Veltmann scheme. The NLO matching coefficient \mathcal{I} for the beam function is found to be

$$\begin{aligned}
\mathcal{I}_{gg}^{(1)}(z) &= \frac{\alpha_s(\mu)C_A}{2\pi} \left(4 \log \frac{\mu}{p_T^{\text{veto}}} \log \frac{\nu}{\bar{n}\cdot p} \delta(1-z) - 2\tilde{p}_{gg}(z) \log \frac{\mu}{p_T^{\text{veto}}} \right), \\
\mathcal{I}_{qq}^{(1)}(z) &= \frac{\alpha_s(\mu)C_F}{2\pi} \left(4 \log \frac{\mu}{p_T^{\text{veto}}} \log \frac{\nu}{\bar{n}\cdot p} \delta(1-z) - 2\tilde{p}_{qq}(z) \log \frac{\mu}{p_T^{\text{veto}}} + (1-z) \right), \\
\mathcal{I}_{gq}^{(1)}(z) &= \frac{\alpha_s(\mu)C_F}{2\pi} \left(-2p_{gq}(z) \log \frac{\mu}{p_T^{\text{veto}}} + z \right), \\
\mathcal{I}_{qg}^{(1)}(z) &= \frac{\alpha_s(\mu)T_F}{2\pi} \left(-2p_{qg}(z) \log \frac{\mu}{p_T^{\text{veto}}} + 2z(1-z) \right),
\end{aligned} \tag{34}$$

with

$$\begin{aligned}
\tilde{p}_{gg}(z) &= \frac{2z}{(1-z)_+} + 2z(1-z) + 2\frac{1-z}{z}, \\
\tilde{p}_{qq}(z) &= \frac{1+z^2}{(1-z)_+}, \\
p_{gq}(z) &= \frac{1+(1-z)^2}{z}, \\
p_{qg}(z) &= 1-2z+2z^2.
\end{aligned} \tag{35}$$

From these fixed order calculations, we can determine the anomalous dimensions used for RG evolution. The anomalous dimension for the jet function is given by

$$\gamma_{J_i} = 2\Gamma_{\text{cusp}} T_i^2 \log \frac{\mu}{p_T^{J_i} R} + \gamma_{J_i}. \tag{36}$$

For the beam function, it is

$$\begin{aligned}
\gamma_B^\nu &= 2\Gamma_{\text{cusp}} T_i^2 \log \frac{\mu}{p_T^{\text{veto}}}, \\
\gamma_B^\mu &= 2\Gamma_{\text{cusp}} T_i^2 \log \frac{\nu}{\bar{n}\cdot p} + \gamma_{B_i},
\end{aligned} \tag{37}$$

where $T_i^2 = C_A$ for gluon and $T_i^2 = C_F$ for quark. Here,

$$\Gamma_{\text{cusp}} = \frac{\alpha_s}{4\pi} \Gamma_0 + \left(\frac{\alpha_s}{4\pi} \right)^2 \Gamma_1 + \dots \tag{38}$$

B RG evolution

The evolutions of the jet and the beam functions are given by

$$\begin{aligned}\mathcal{R}_{J_i} &= \exp \left[-2T_i^2 S(\mu_J, \mu) - A_{J_i}(\mu_J, \mu) \right] \left(\frac{\mu_J}{p_T^{J_i} R} \right)^{-2T_i^2 A_\Gamma(\mu_J, \mu)}, \\ U_{B,a} &= \exp \left[-T_a^2 A_\Gamma(p_T^{veto}, \mu) \log \frac{\nu^2}{\nu_B^2} \right] \exp \left[-T_a^2 A_\Gamma(\mu_B, \mu) \log \frac{\nu_B^2}{\omega_a^2} - A_{B_a}(\mu_B, \mu) \right].\end{aligned}\quad (39)$$

We have defined $\mathcal{I}_{B,a,b} = U_{B,a} U_{B,b}$ in Eqs. (26) and (27). For the Higgs production process considered in this work, we have, the following color identities: for the ggg channel, $T_i \cdot T_j = -C_A/2$; for the $q_1 \bar{q}_2 g_3$ channel, $T_1 \cdot T_2 = -(C_F - C_A/2)$ and $T_1 \cdot T_3 = T_2 \cdot T_3 = -C_A/2$. The anomalous dimension for the hard function can be found in Ref. [32]. The solution to the RG equation is

$$\begin{aligned}U_H &= \exp \left[2 \sum_i T_i^2 S(\mu_H, \mu) - 2A_H(\mu_H, \mu) + 2A_\Gamma(\mu_H, \mu) \sum_{i \neq j} \frac{T_i \cdot T_j}{2} \log \Delta R_{ij}^2 \right] \\ &\times \prod_i \left(\frac{\mu_H}{\omega_i} \right)^{2T_i^2 A_\Gamma(\mu_H, \mu)},\end{aligned}\quad (40)$$

where $\Delta R_{ij}^2 = 2(\cosh(\Delta\eta_{ij}) - \cos(\Delta\phi_{ij}))$ for $i, j \neq a, b$, $\Delta R_{ia}^2 = e^{-\eta_i}$, $\Delta R_{ib}^2 = e^{\eta_i}$ and $\Delta R_{ab}^2 = 1$. Also $\omega_i = p_T^i$ if $i \in J$, otherwise $\omega_a = x_a \sqrt{s}$. The soft anomalous dimension is determined by the consistency relation in Eq. (24), which gives the solution

$$\begin{aligned}U_S &= \exp \left[-2 \sum_{i \in B} T_i^2 S(\mu_s, \mu) - A_s(\mu_s, \mu) - 2A_\Gamma(\mu_s, \mu) \sum_{i \neq j} \frac{T_i \cdot T_j}{2} \log \Delta R_{ij}^2 \right] \\ &\times \left(\frac{1}{R} \right)^{\sum_{i \in J} 2T_i^2 A_\Gamma(\mu_s, \mu)} \left(\frac{\nu_s}{\mu_s} \right)^{\sum_{i \in B} 2T_i^2 A_\Gamma(\mu_s, \mu)} \left(\frac{\nu}{\nu_s} \right)^{\sum_{i \in B} 2T_i^2 A_\Gamma(p_T^{veto}, \mu)}.\end{aligned}\quad (41)$$

For the NLL resummation, we need

$$A_\Gamma(\mu_i, \mu_f) = \frac{\Gamma_0}{2\beta_0} \left\{ \log r + \frac{\alpha_s(\mu_i)}{4\pi} \left(\frac{\Gamma_1}{\Gamma_0} - \frac{\beta_1}{\beta_0} \right) (r - 1) \right\}, \quad (42)$$

and

$$S(\mu_i, \mu_f) = \frac{\Gamma_0}{4\beta_0^2} \left\{ \frac{4\pi}{\alpha_s(\mu_i)} \left(1 - \frac{1}{r} - \log r \right) + \left(\frac{\Gamma_1}{\Gamma_0} - \frac{\beta_1}{\beta_0} \right) (1 - r + \log r) + \frac{\beta_1}{2\beta_0} \log^2 r \right\}, \quad (43)$$

where $r = \alpha_s(\mu_f)/\alpha_s(\mu_i)$ and

$$\beta_0 = \frac{11}{3}C_A - \frac{4}{3}T_F n_f, \quad (44)$$

$$\beta_1 = \frac{34}{3}C_A^2 - \frac{20}{3}C_A T_F n_f - 4C_F T_F n_f, \quad (45)$$

$$\Gamma_0 = 4, \quad (46)$$

$$\Gamma_1 = 4 \left[C_A \left(\frac{67}{9} - \frac{\pi^2}{3} \right) - \frac{20}{9} T_F n_f \right]. \quad (47)$$

$A_{J/B}$, A_H and A_S are needed at leading order, and can be obtained by substituting the Γ_0 in A_Γ with the corresponding γ_0 and expanding in α_s . For $A_{J/B}$ we have

$$\gamma_0^{J^a} = 6C_F, \quad (48)$$

and

$$\gamma_0^{J^g} = 2\beta_0, \quad (49)$$

for quark and gluon jets or beam functions, respectively. For $\gamma_H = \sum_i \gamma_i$, we have

$$\gamma_0^a = -3C_F, \quad (50)$$

and

$$\gamma_0^g = -\beta_0, \quad (51)$$

The two loop γ_S can be extracted via the relation $2\gamma_H + \gamma_{J_i} + \gamma_S + \gamma_{B_a} + \gamma_{B_b} = 0$. At one loop, $\gamma_0^S = 0$.

C Expanded results

Expanding out the resummed result will give us the fixed order singular term up to NLL. We find

$$\frac{H}{H_0} = 1 + \frac{\alpha_s(\mu)}{4\pi} \left(-\frac{\Gamma_0}{2} \sum_i T_i^2 \frac{L^2}{2} + \left(-\Gamma_0 \sum_{i \neq j} \frac{T_i \cdot T_j}{2} \log \Delta R_{ij}^2 - \Gamma_0 \sum_i T_i^2 \log \frac{\mu_H}{\omega_i} + \gamma_0^H + n\beta_0 \right) L \right), \quad (52)$$

where we have assumed at the leading order $H_0 \propto \alpha_s^n$ and defined $L = \log(\mu/\mu_H)^2$ where μ_H is of order p_T^J , and ΔR_{ij}^2 and ω_i have been defined previously.

The expanded jet evolution gives

$$J_i = 1 + \frac{\alpha_s(\mu)}{4\pi} \left(\frac{\Gamma_0}{2} T_i^2 \frac{L^2}{2} + \left(\Gamma_0 T_i^2 \log \frac{\mu_J}{p_T^J R} + \frac{\gamma_0^{J_i}}{2} \right) L \right), \quad (53)$$

where $L = \log(\mu/\mu_j)^2$. We have checked that it reproduces singular pieces of the fixed-order NLO calculation of the jet function. To see this we note that the first two NLO terms can be combined to give $\frac{\Gamma_0 T_i^2 \log^2 \frac{\mu^2}{(p_T^i R)^2} + \mathcal{O}(\lambda^0)$ as long as μ_J is of order $p_T^{J_i} R$.

The singular terms of the beam coefficient are given by

$$\begin{aligned} \mathcal{I}_{aa'}(z) = & \delta(1-z)\delta_{aa'} \left(1 + \frac{\alpha_s(\mu)}{4\pi} \left[\Gamma_0 T_a^2 \left(\log \frac{\mu}{p_T^{veto}} \log \frac{\nu^2}{\nu_B^2} + \log \frac{\mu}{\mu_B} \log \frac{\nu_B^2}{\omega_a^2} \right) + \gamma_0^{B_a} \log \frac{\mu}{\mu_B} \right] \right) \\ & - \frac{\alpha_s(\mu)}{\pi} p_{aa'}(z) \log \frac{\mu}{\mu_B}, \end{aligned} \quad (54)$$

where $p_{aa'}(z)$ is the normal splitting function. This result again agrees with the fixed order calculation if we choose $\mu_B \sim p_T^{veto}$ and $\nu_B \sim \omega_a$.

Finally, the soft function is

$$\begin{aligned} S = & 1 + \frac{\alpha_s(\mu)}{4\pi} \left(\frac{\Gamma_0}{2} \sum_{a \in B} T_a^2 \left[\frac{L^2}{2} + \log \frac{\nu_S^2}{\nu^2} \log \frac{\mu^2}{(p_T^{veto})^2} \right] \right) \\ & + \frac{\alpha_s(\mu)}{4\pi} \left(\frac{\Gamma_0}{2} \sum_{i \in J} T_i^2 \log R^2 + \frac{\Gamma_0}{2} \sum_{a \in B} T_a^2 \log \frac{\mu_S^2}{\nu_S^2} + \Gamma_0 \sum_{i \neq j} \frac{T_i \cdot T_j}{2} \log \Delta R_{ij}^2 + \frac{\gamma_0^S}{2} \right) L, \end{aligned} \quad (55)$$

where $L = \log(\mu/\mu_S)^2$ and $\mu_S \sim \nu_S \sim p_T^{veto}$. We note that once we combine the soft and the beam functions, the ν dependence in these two contributions cancels, as required. If we set $\mu_B = \mu_S = p_T^{veto}$, the ν_S and ν_B dependence also disappear. We note that numerically, the $\log R^2 \times L$ term is of order $0.1 \times L$, which we interpret as a single-log term.

References

- [1] G. Aad *et al.* [ATLAS Collaboration], Phys. Lett. B **716**, 62 (2012) [arXiv:1206.0756 [hep-ex]].
- [2] S. Chatrchyan *et al.* [CMS Collaboration], Phys. Lett. B **710**, 91 (2012) [arXiv:1202.1489 [hep-ex]].
- [3] C. Anastasiou, G. Dissertori, F. Stockli and B. R. Webber, JHEP **0803**, 017 (2008) [arXiv:0801.2682 [hep-ph]].
- [4] I. W. Stewart and F. J. Tackmann, Phys. Rev. D **85**, 034011 (2012) [arXiv:1107.2117 [hep-ph]].
- [5] A. Banfi, G. P. Salam and G. Zanderighi, JHEP **1206**, 159 (2012) [arXiv:1203.5773 [hep-ph]].

- [6] I. W. Stewart, F. J. Tackmann and W. J. Waalewijn, Phys. Rev. Lett. **105**, 092002 (2010) [arXiv:1004.2489 [hep-ph]].
- [7] X. Liu, S. Mantry and F. Petriello, arXiv:1205.4465 [hep-ph].
- [8] T. Becher and M. Neubert, JHEP **1207**, 108 (2012) [arXiv:1205.3806 [hep-ph]].
- [9] A. Banfi, P. F. Monni, G. P. Salam and G. Zanderighi, arXiv:1206.4998 [hep-ph].
- [10] F. J. Tackmann, J. R. Walsh and S. Zuberi, arXiv:1206.4312 [hep-ph].
- [11] C. F. Berger, C. Marcantonini, I. W. Stewart, F. J. Tackmann and W. J. Waalewijn, JHEP **1104**, 092 (2011) [arXiv:1012.4480 [hep-ph]].
- [12] A. Banfi, G. P. Salam and G. Zanderighi, JHEP **1006**, 038 (2010) [arXiv:1001.4082 [hep-ph]].
- [13] J. M. Campbell and R. K. Ellis, Nucl. Phys. Proc. Suppl. **205-206**, 10 (2010) [arXiv:1007.3492 [hep-ph]].
- [14] C. W. Bauer, S. Fleming and M. E. Luke, Phys. Rev. D **63**, 014006 (2000) [hep-ph/0005275].
- [15] C. W. Bauer, S. Fleming, D. Pirjol, and I. W. Stewart, Phys. Rev. **D63**, 114020 (2001), hep-ph/0011336.
- [16] C. W. Bauer and I. W. Stewart, Phys. Lett. B **516**, 134 (2001) [hep-ph/0107001].
- [17] C. W. Bauer, D. Pirjol, and I. W. Stewart, Phys. Rev. **D65**, 054022 (2002), hep-ph/0109045.
- [18] C. W. Bauer, S. Fleming, D. Pirjol, I. Z. Rothstein, and I. W. Stewart, Phys. Rev. **D66**, 014017 (2002), hep-ph/0202088.
- [19] G. Aad *et al.* [ATLAS Collaboration], Phys. Lett. B **716**, 1 (2012) [arXiv:1207.7214 [hep-ex]].
- [20] S. Chatrchyan *et al.* [CMS Collaboration], Phys. Lett. B **716**, 30 (2012) [arXiv:1207.7235 [hep-ex]].
- [21] M. Cacciari, G. P. Salam and G. Soyez, JHEP **0804**, 063 (2008) [arXiv:0802.1189 [hep-ph]].
- [22] J. R. Walsh and S. Zuberi, arXiv:1110.5333 [hep-ph].
- [23] S. D. Ellis, A. Hornig, C. Lee, C. K. Vermilion and J. R. Walsh, Phys. Lett. B **689**, 82 (2010) [arXiv:0912.0262 [hep-ph]].
- [24] Y. -T. Chien, R. Kelley, M. D. Schwartz and H. X. Zhu, arXiv:1208.0010 [hep-ph].

- [25] A. V. Manohar and I. W. Stewart, Phys. Rev. D **76**, 074002 (2007) [hep-ph/0605001].
- [26] J. -Y. Chiu, A. Jain, D. Neill and I. Z. Rothstein, JHEP **1205**, 084 (2012) [arXiv:1202.0814 [hep-ph]].
- [27] S. Mantry and F. Petriello, Phys. Rev. D **81**, 093007 (2010) [arXiv:0911.4135 [hep-ph]].
- [28] T. Becher and G. Bell, Phys. Lett. B **713**, 41 (2012) [arXiv:1112.3907 [hep-ph]].
- [29] M. Dasgupta and G. P. Salam, Phys. Lett. B **512**, 323 (2001) [hep-ph/0104277].
- [30] C. R. Schmidt, Phys. Lett. B **413**, 391 (1997) [hep-ph/9707448].
- [31] A. D. Martin, W. J. Stirling, R. S. Thorne and G. Watt, Eur. Phys. J. C **64**, 653 (2009) [arXiv:0905.3531 [hep-ph]].
- [32] R. Kelley and M. D. Schwartz, Phys. Rev. D **83**, 045022 (2011) [arXiv:1008.2759 [hep-ph]].